

A two-step control approach for docking of autonomous underwater vehicles

Pedro Batista^{1,*}, Carlos Silvestre^{1,2} and Paulo Oliveira^{1,3}

¹*Institute for Systems and Robotics, Instituto Superior Técnico, Universidade de Lisboa, Lisboa, Portugal*

²*Department of Electrical and Computer Engineering, Faculty of Science and Technology, University of Macau, Taipa, Macau*

³*Department of Mechanical Engineering, Instituto Superior Técnico, Universidade de Lisboa, Lisboa, Portugal*

SUMMARY

This paper presents a novel integrated guidance and control strategy for docking of autonomous underwater vehicles. The approach to the base, and hence the control design, is divided in two steps: (i) in the first, at higher speed, the vehicle dynamics is assumed to be underactuated, and an appropriate control law is derived to steer the vehicle towards the final docking path, achieving convergence to zero of the appropriate error variables for almost all initial conditions; (ii) in the second stage, at low speed, the vehicle is assumed to be fully actuated, and a robust control law is designed that achieves convergence to zero of the appropriate error variables for all initial conditions, in the presence of parametric model uncertainty. Simulations are presented illustrating the performance of the proposed controllers, including model uncertainty and sensor noise. Copyright © 2014 John Wiley & Sons, Ltd.

Received 21 December 2012; Revised 10 January 2014; Accepted 10 January 2014

KEY WORDS: docking; autonomous underwater vehicles; nonlinear control

1. INTRODUCTION

The European Union project TRIDENT aims to develop an intervention autonomous underwater vehicle (AUV) to perform several tasks such as seabed surveying or intervention operations, after which the vehicle is expected to autonomously return and dock to its base station. This problem, commonly referred to as docking, is one of the many challenges that the design of AUVs entails, and it is one of the key enabling features of AUVs, providing the means to return to a base station to perform vital activities such that recharging batteries, transferring data, changing the payload, and downloading new mission parameters.

The initial approach to the base, usually denominated as homing, is not considered in this paper, see [1, 2], and references therein for further details on that subject. During the homing stage, the only purpose of the vehicle is to approach the vicinity of the base, without any particular attitude or direction of arrival. In the docking approach, the vehicle approaches the base along a particular path, with a particular direction of arrival. Previous work in the literature on the docking problem can be found in [3], where a simple terminal guidance system is proposed based upon an optical quadrant tracker that locks onto a visible light source, which requires good visibility conditions. An alternative based on an electromagnetic homing system is presented in [4], whereas in [5], a visual servo controller approach is proposed. More recently, in [6], the concept of optical terminal

*Correspondence to: Pedro Batista, Institute for Systems and Robotics, Instituto Superior Técnico, Universidade de Lisboa, Lisboa, Portugal.

†E-mail: pbatista@isr.ist.utl.pt

guidance is recovered, whereas in [7], a sliding mode control strategy is detailed to solve the homing and docking problems.

The main contribution of this paper is the development of two integrated guidance and control laws to solve the docking problem based upon ultra-short baseline (USBL) acoustic positioning system measurements, which provides the positions of two transponders that are fixed to the base station. With the proposed strategy, the problem is divided in two stages: (i) in the initial approach, the vehicle dynamics are assumed to be underactuated, which poses its own challenges, and the goal is to simply drive the vehicle towards an appropriate docking path, which is defined as a straight line that passes through the middle point between the transponders and that is orthogonal to the direction defined by these two transponders; and (ii) in the final approach, which is carried out at a lower speed, the vehicle employs a more efficient thruster to generate transversal force, which allows to consider fully actuated dynamics. In this case, and because the desired docking profile should be followed with great accuracy, an adaptive control law is proposed that accounts for uncertainty in the hydrodynamic parameters, which are often not known with enough accuracy, as opposed to other parameters like the mass and the inertia of the vehicle. Finally, the problem is considered only in the horizontal plane, as in this stage, the vehicle is usually vertically stabilized by an independent controller resorting to a depth sensor. Note that the derivation of the integrated guidance and control law could be extended to the 3D case, which would, however, result in a much more intricate convergence analysis for the initial docking approach, with no significant differences in the final approach. It is important to stress that there is no switching back and forth between the two control laws: once the final docking controller is engaged, there is no switching back to the initial docking controller. In addition, the final docking controller ensures convergence to zero of all appropriate error variables for all initial conditions. As such, no further stability issues need to be addressed. Previous work by the authors can be found in [8], where the proposed docking solution was first introduced. The present work presents extended proofs and includes more detailed simulation results with sensor noise in order to assess the performance in realistic environments.

The paper is organized as follows. Section 2 presents the problem at hand, while Section 3 details the control design and stability analysis for both stages of the docking approach. Simulation results are presented in Section 4 to evaluate the performance of the proposed solutions, and some concluding remarks are provided in Section 5.

2. PROBLEM STATEMENT

Consider an autonomous underwater vehicle moving in the horizontal plane. Let $\{I\}$ be an inertial reference frame and $\{B\}$ a reference frame attached to the vehicle, whose origin is located at the center of mass of the vehicle, usually denominated in the literature as the body-fixed reference frame. Let $\mathbf{p}(t) \in \mathbb{R}^2$ denote the position of the origin of $\{B\}$, described in $\{I\}$, $\mathbf{v}(t) = [u(t) \ v(t)]^T \in \mathbb{R}^2$ the linear velocity of the vehicle relative to $\{I\}$, expressed in body-fixed coordinates, where $u(t)$ and $v(t)$ are the surge and sway velocities, respectively, and $\omega(t)$ the angular velocity of the vehicle, expressed in $\{B\}$. The vehicle kinematics are given by

$$\dot{\mathbf{p}}(t) = \mathbf{R}(t)\mathbf{v}(t), \quad (1)$$

where $\mathbf{R}(t)$ denotes the rotation matrix from body-fixed to inertial coordinates, which satisfies $\dot{\mathbf{R}}(t) = \mathbf{R}(t)\mathbf{S}[\omega(t)]$, where $\mathbf{S}(\cdot)$ is the skew-symmetric matrix

$$\mathbf{S}(x) = \begin{bmatrix} 0 & -x \\ x & 0 \end{bmatrix}.$$

2.1. Initial docking approach

The idea during the initial docking approach is to employ the main propellers of the vehicle, at a certain cruise speed, to drive the vehicle toward the final docking path. As such, the vehicle is

assumed to be underactuated during this stage. The dynamic equations of motion, in the horizontal plane, of an underactuated autonomous underwater vehicle can be written as [9, 10]

$$\begin{cases} \dot{u}(t) = -\frac{D_u+d_u[|u(t)|]}{M_u}u(t) + v(t)\omega(t) + \frac{1}{M_u}\tau_u(t) \\ \dot{v}(t) = -\frac{D_v+d_v[|v(t)|]}{M_v}v(t) - u(t)\omega(t) \\ \dot{\omega}(t) = -\frac{D_\omega+d_\omega[|\omega(t)|]}{J}\omega(t) + \frac{1}{J}\tau_\omega(t) \end{cases}, \quad (2)$$

where $M_u > 0$ and $M_v > 0$ represent the mass of the vehicle, including added mass effects, $J > 0$ denotes the inertia of the vehicle, $D_u > 0$, $D_v > 0$, $D_\omega > 0$ are hydrodynamic damping parameters, $d_u[|u(t)|] : \mathbb{R}_0^+ \rightarrow \mathbb{R}_0^+$, $d_v[|v(t)|] : \mathbb{R}_0^+ \rightarrow \mathbb{R}_0^+$, and $d_\omega[|\omega(t)|] : \mathbb{R}_0^+ \rightarrow \mathbb{R}_0^+$ are positive functions that capture higher order hydrodynamic damping effects, $\tau_u(t) \in \mathbb{R}$ is the control force along the surge motion of the vehicle, and $\tau_\omega(t) \in \mathbb{R}$ is the angular motion control torque.

Suppose that there exist two transponders fixed in the mission scenario, equally spaced from the final docking position, as depicted in Figure 1. One of the transponders is designated as the left transponder, whereas the other is the right transponder, whose inertial positions are denoted by ${}^I\mathbf{t}_l \in \mathbb{R}^2$ and ${}^I\mathbf{t}_r \in \mathbb{R}^2$, respectively. The first problem considered here is to drive the underactuated AUV toward the path that passes through the docking position and is orthogonal to the straight line defined by the two transponders, shortening the distance to the docking position, as suggested in Figure 1. The vehicle is assumed to be equipped with a navigation system, that provides its linear and angular velocity, and an Ultra-short Baseline positioning system that gives the position of the transponders with respect to the vehicle, expressed in body-fixed coordinates, as given by

$$\mathbf{t}_l(t) = \mathbf{R}^T(t) [{}^I\mathbf{t}_l - \mathbf{p}(t)]$$

and

$$\mathbf{t}_r(t) = \mathbf{R}^T(t) [{}^I\mathbf{t}_r - \mathbf{p}(t)],$$

see, for example, [1].

2.2. Final docking approach

In the final docking approach, the goal is similar to the one previously presented. However, it is carried out at a much lower speed and the vehicle eventually reaches the docking position. In this case, the full actuation capabilities of the vehicle are exploited, and robustness to model uncertainties is essential so that the vehicle follows exactly a predefined straight line trajectory profile, avoiding collisions with the docking station.

The dynamics of an AUV depend on several physical parameters, some of which are often only known with large uncertainty. Whereas the added mass and inertia terms can be determined with reasonable confidence, the hydrodynamic damping terms are usually difficult to identify or quantify.

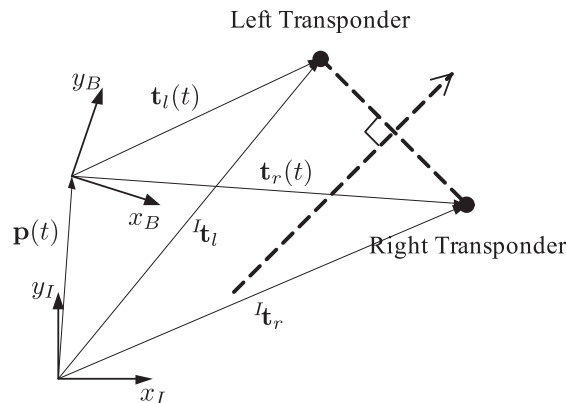


Figure 1. Initial docking approach scenario.

As such, an adaptive controller should be designed. Considering that the hydrodynamic coefficients are constant, it is possible to rewrite the hydrodynamic damping terms in (2) as

$$\begin{bmatrix} D_u + d_u[|u(t)|] \\ D_v + d_v[|v(t)|] \end{bmatrix} = \phi_v^T[\mathbf{v}(t)]\psi_v$$

and

$$D_\omega + d_\omega[|\omega(t)|] = \phi_\omega^T[\omega(t)]\psi_\omega,$$

where $\phi_v[\mathbf{v}(t)] \in \mathbb{R}^{n_v \times 2}$ and $\phi_\omega[\omega(t)] \in \mathbb{R}^{n_\omega}$ are known functions of $\mathbf{v}(t)$ and $\omega(t)$, respectively, and $\psi_v \in \mathbb{R}^{n_v}$ and $\psi_\omega \in \mathbb{R}^{n_\omega}$ are the hydrodynamic damping coefficients, only known up to some error, see, for example, [11]. Considering a fully actuated AUV moving in the horizontal plane, the dynamic equations of motion can then be written, in compact form, as

$$\begin{cases} \mathbf{M}\dot{\mathbf{v}}(t) = -\mathbf{S}[\omega(t)]\mathbf{M}\mathbf{v}(t) - \phi_v^T[\mathbf{v}(t)]\psi_v + \boldsymbol{\tau}_v(t) \\ J\dot{\omega}(t) = -\phi_\omega[\omega(t)]^T\psi_\omega + \tau_\omega(t), \end{cases} \quad (3)$$

where $\mathbf{M} = \text{diag}(M_u, M_v) \in \mathbb{R}^{2 \times 2}$ is the added-mass matrix and $\boldsymbol{\tau}_v(t) = [\tau_u(t) \ \tau_v(t)]^T \in \mathbb{R}^2$ is the full control force input.

Consider the final docking scenario as depicted in Figure 2, where $l_x(t) \in \mathbb{R}$ denotes the distance to the docking position along the final docking path, $l_y(t) \in \mathbb{R}$ denotes the minimum distance from the vehicle to docking path, and $\alpha_1(t)$ denotes the error of orientation of the vehicle with respect to the docking path. Further consider a smooth desired distance profile along the docking path $l_{xd}(t) \in \mathbb{R}$. The problem considered here is that of designing an adaptive control law so that $l_x(t)$ converges to $l_{xd}(t)$ and both $l_y(t)$ and $\alpha_1(t)$ converge to zero, considering that the hydrodynamic coefficients ψ_v and ψ_ω are unknown.

2.3. Alternative sensor suite

In the framework previously introduced, two transponders are required in the docking station. However, it is possible to redefine the docking problem considering a single transponder, whose inertial position is denoted by ${}^I\mathbf{t}_s \in \mathbb{R}^2$, and an inertial direction of arrival ${}^I\mathbf{d} \in \mathbb{R}^2$ orthogonal to the line defined by the two transponders, given by

$${}^I\mathbf{t}_s = \frac{{}^I\mathbf{t}_l + {}^I\mathbf{t}_r}{2}$$

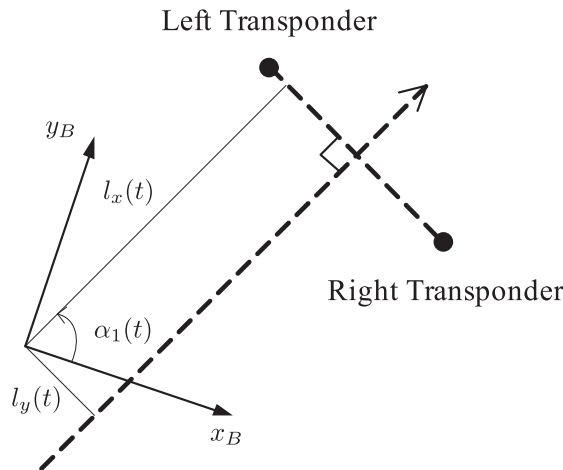


Figure 2. Final docking approach scenario.

and

$${}^I\mathbf{d} = \frac{\mathbf{S}(1) [{}^I\mathbf{t}_l - {}^I\mathbf{t}_r]}{\|\mathbf{S}(1) [{}^I\mathbf{t}_l - {}^I\mathbf{t}_r]\|},$$

respectively. In practical situations, the direction of arrival could be known a priori (fixed base) or transmitted prior to the docking operation of the AUV. To these new inertial vectors correspond body-fixed vectors

$$\mathbf{t}_s(t) = \frac{\mathbf{t}_l(t) + \mathbf{t}_r(t)}{2}$$

and

$$\mathbf{d}(t) = \frac{\mathbf{S}(1)[\mathbf{t}_l(t) - \mathbf{t}_r(t)]}{\|\mathbf{S}(1)[\mathbf{t}_l(t) - \mathbf{t}_r(t)]\|},$$

respectively, as available to the AUV. Notice that the left and right transponder measurements can be readily obtained, as given by

$$\mathbf{t}_l(t) = \mathbf{t}_s(t) - \frac{L_t}{2}\mathbf{S}(1)\mathbf{d}(t)$$

and

$$\mathbf{t}_r(t) = \mathbf{t}_s(t) + \frac{L_t}{2}\mathbf{S}(1)\mathbf{d}(t),$$

respectively. Notice that, from the theoretical point of view, the use of two transponders or one transponder and one direction of arrival is equivalent.

3. CONTROLLER DESIGN AND STABILITY ANALYSIS

3.1. Initial docking approach

This section details the design and stability analysis of a control law for the initial docking approach of an underactuated AUV towards a base station. Essentially, a desired velocity is first determined such that if the vehicle followed this velocity, the control goal would be achieved. Then, the angular speed of the vehicle is reworked so that the desired velocity is attained. In the end, the force along the surge axis and the torque are determined so that the surge speed and the angular velocities converge to the desired values, which in turn ensures that all errors converge to zero. The idea of setting a desired velocity first and then using the angular speed to achieve this goal has been used before, see, for example, [12], [1, 2], and [13]. The latter presents a path following algorithm for underactuated marine surface vessels, including the dynamics of the vehicle and known constant ocean currents.

In order to derive the control law notice that, when the vehicle is moving along the final docking path, the distance between the vehicle and each transponder is identical. That suggests the definition of the error variable

$$z_1(t) := \|\mathbf{t}_l(t)\|^2 - \|\mathbf{t}_r(t)\|^2. \tag{4}$$

Taking the time derivative of (4) gives

$$\dot{z}_1(t) = -2[\mathbf{t}_l(t) - \mathbf{t}_r(t)]^T \mathbf{v}(t).$$

Consider the desired vehicle velocity defined by

$$\mathbf{v}_d(t) := \frac{V_d}{L_t \sqrt{1 + K_1^2 z_1^2(t)}} K_1 z_1(t) [\mathbf{t}_l(t) - \mathbf{t}_r(t)] - \frac{V_d}{L_t \sqrt{1 + K_1^2 z_1^2(t)}} \mathbf{S}(1) [\mathbf{t}_l(t) - \mathbf{t}_r(t)], \tag{5}$$

where $V_d > 0$ is the desired speed of the AUV along the docking path, $K_1 > 0$ is a constant control gain, and $L_t := \|\mathbf{t}_l(t) - \mathbf{t}_r(t)\| = \|\mathbf{t}_l - \mathbf{t}_r\|$ is the distance between the transponders. Clearly, if the linear velocity of the vehicle coincides with $\mathbf{v}_d(t)$, then $z_1(t)$ converges to zero, as one gets

$\dot{z}_1(t) = -\frac{2L_t V_d K_1}{\sqrt{1+K_1^2 z_1^2(t)}} z_1(t)$. In order to achieve this behavior, the first term of (5) would suffice.

However, if the second term of (5) is removed, the speed of the vehicle converges to zero as $z_1(t)$ converges to zero, although the goal is to drive the vehicle along the final docking path. The extra term ensures the desired speed of the vehicle when it is moving along the docking path. Notice also that, in this way, the norm of the desired velocity is constant, namely, $\|\mathbf{v}_d(t)\| = V_d$ for all t . Long but straightforward computations allow to show that the derivative of (5), which is required in the ensuing, can be written as

$$\dot{\mathbf{v}}_d(t) = -\left(\omega(t) + \frac{2K_1[\mathbf{t}_l(t) - \mathbf{t}_r(t)]^T \mathbf{v}(t)}{1 + K_1^2 z_1^2(t)}\right) \mathbf{S}(1) \mathbf{v}_d(t). \quad (6)$$

In order to derive a control law that ensures that the linear velocity of the vehicle, $\mathbf{v}(t)$, converges to the desired linear velocity, $\mathbf{v}_d(t)$, consider the error variables

$$z_2(t) := u(t) - V_d \quad (7)$$

and

$$\mathbf{z}_3(t) := \mathbf{v}_d(t) - \begin{bmatrix} V_d \\ 0 \end{bmatrix}. \quad (8)$$

Looking into these definitions, one concludes that, in the absence of sway velocity and with positive surge speed, $\mathbf{v}_d(t) = \mathbf{v}(t)$ if and only if $u(t) = V_d$ and $\mathbf{v}_d(t) = [V_d \ 0]^T$ or, equivalently, $z_2(t) = 0$ and $\mathbf{z}_3(t) = \mathbf{0}$. Even though the sway velocity is not constrained by these error variables, it will be shown, in the ensuing, that with the control law based upon these two error variables, not only do $z_2(t)$ and $\mathbf{z}_3(t)$ converge to zero but the sway velocity also converges to zero, which implies that the velocity of the vehicle converges to the desired velocity. The derivation of the control law follows, considering standard Lyapunov and backstepping techniques.

The time derivative of (7) is given by $\dot{z}_2(t) = \dot{u}(t)$, which using (2) can be written as

$$\dot{z}_2(t) = -\frac{D_u + d_u[|u(t)|]}{M_u} u(t) + v(t)\omega(t) + \frac{1}{M_u} \tau_u(t).$$

Let

$$\tau_u(t) = (D_u + d_u[|u(t)|])u(t) - M_u v(t)\omega(t) - M_u K_2 z_2(t), \quad (9)$$

where $K_2 > 0$ is a constant control gain. Then, the derivative of $z_2(t)$ becomes $\dot{z}_2(t) = -K_2 z_2(t)$, which readily allows to conclude that $z_2(t)$ converges globally exponentially fast to zero.

The time derivative of (8) can be written, using (6), as

$$\dot{\mathbf{z}}_3(t) = -\left(\omega(t) + \frac{2K_1[\mathbf{t}_l(t) - \mathbf{t}_r(t)]^T \mathbf{v}(t)}{1 + K_1^2 z_1^2(t)}\right) \mathbf{S}(1) \mathbf{v}_d(t). \quad (10)$$

If the angular velocity is set equal to

$$\omega_d(t) := -\frac{2K_1[\mathbf{t}_l(t) - \mathbf{t}_r(t)]^T \mathbf{v}(t)}{1 + K_1^2 z_1^2(t)} + K_3 [0 \ 1] \mathbf{v}_d(t), \quad (11)$$

where $K_3 > 0$ is a constant control gain, then $z_3(t)\dot{z}_3(t)$ becomes negative semidefinite. However, the angular velocity is not an actual control variable. As such, the standard backstepping technique is employed to extend the control law to the dynamics of the vehicle. To that purpose, consider the additional error variable

$$z_4(t) := \omega(t) - \omega_d(t) \quad (12)$$

and define the Lyapunov candidate function

$$V_1(t) := \frac{1}{2} \|\mathbf{z}_3(t)\|^2 + \frac{1}{2} z_4^2(t). \quad (13)$$

The time derivative of (13) is given by

$$\dot{V}_1(t) = \mathbf{z}_3^T(t)\dot{\mathbf{z}}_3(t) + z_4(t)\dot{z}_4(t). \tag{14}$$

Using (11) and (12) in (10) and taking the time derivative of (12), using (2) and (8) also, allows to rewrite (14) as

$$\begin{aligned} \dot{V}_1(t) &= -[z_4(t) + K_3 [0 \ 1]\mathbf{v}_d(t)] \mathbf{z}_3^T(t)\mathbf{S}(1)\mathbf{v}_d(t) \\ &\quad + z_4(t) \left[-\frac{D_\omega + d_\omega[|\omega(t)|]}{J}\omega(t) + \frac{1}{J}\tau_\omega(t) - \dot{\omega}_d(t) \right] \\ &= -V_d z_4(t)[0 \ 1]\mathbf{z}_3(t) - K_3 V_d [[0 \ 1]\mathbf{z}_3(t)]^2 \\ &\quad + z_4(t) \left[-\frac{D_\omega + d_\omega[|\omega(t)|]}{J}\omega(t) + \frac{1}{J}\tau_\omega(t) - \dot{\omega}_d(t) \right], \end{aligned}$$

where

$$\begin{aligned} \dot{\omega}_d &= -\frac{2K_1[\mathbf{t}_l(t) - \mathbf{t}_r(t)]^T \mathbf{S}[\omega(t)]\mathbf{v}(t) + 2K_1[\mathbf{t}_l(t) - \mathbf{t}_r(t)]^T \dot{\mathbf{v}}(t)}{1 + K_1^2 z_1^2(t)} \\ &\quad - \frac{8K_1^3 z_1(t)([\mathbf{t}_l(t) - \mathbf{t}_r(t)]^T \mathbf{v}(t))^2}{[1 + K_1^2 z_1^2(t)]^2} + K_3[0 \ 1]\dot{\mathbf{v}}_d(t), \end{aligned}$$

with

$$\dot{\mathbf{v}}(t) = \left[\begin{array}{c} -K_2 z_2(t) \\ -\frac{D_v + d_v[|v(t)|]}{M_v}v(t) - u(t)\omega(t) \end{array} \right].$$

Setting

$$\tau_\omega(t) = (D_\omega + d_\omega[|\omega(t)|])\omega(t) + J[\dot{\omega}_d(t) + V_d [0 \ 1]\mathbf{z}_3(t) - K_4 z_4(t)] \tag{15}$$

yields

$$\dot{V}_1(t) = -K_3 V_d [[0 \ 1]\mathbf{z}_3(t)]^2 - K_4 z_4^2(t), \tag{16}$$

which is negative semidefinite.

The following proposition establishes the convergence of the error variables $z_2(t)$, $\mathbf{z}_3(t)$, and $z_4(t)$ to zero.

Proposition 1

Consider an underactuated AUV moving in the horizontal plane in a mission scenario as described in Section 2.1, with kinematics and dynamics given by (1) and (2), respectively. Then, with the control law (9) and (15), $z_2 = 0$ is a globally exponentially stable equilibrium point and $\mathbf{z}_3 = \mathbf{0}$, $z_4 = 0$ is an almost globally asymptotically stable equilibrium point.

Proof

The fact that $z_2(t)$ converges globally exponentially fast to zero is trivially concluded, as with the control law (9), it follows that $\dot{z}_2(t) = -K_2 z_2(t)$, where K_2 is a positive constant. With the control law (15), the dynamics of $\mathbf{z}_3(t)$ and $z_4(t)$ can be written as

$$\begin{cases} \dot{\mathbf{z}}_3(t) = -K_3 [0 \ 1]\mathbf{z}_3(t)\mathbf{S}(1)\mathbf{z}_3(t) - V_d K_3 [0 \ 1]\mathbf{z}_3(t) \begin{bmatrix} 0 \\ 1 \end{bmatrix} \\ \quad - z_4(t)\mathbf{S}(1)\mathbf{z}_3(t) - V_d z_4(t) \begin{bmatrix} 0 \\ 1 \end{bmatrix} \\ \dot{z}_4(t) = -K_4 z_4(t) + V_d [0 \ 1]\mathbf{z}_3(t), \end{cases}$$

which is an autonomous system. The Lyapunov function $V_1(t)$ is, by construction, continuous, radially unbounded, and positive definite. With the control law (15), the derivative of $V_1(t)$ can be written as (16), which is negative semidefinite along the trajectories of the system. In fact, the derivative of $V_1(t)$ has two zeros, one coincident with the origin, ($\mathbf{z}_3 = \mathbf{0}$, $z_4 = 0$), and another that corresponds to ($\mathbf{z}_3 = -[2V_d \ 0]^T$, $z_4 = 0$). Locally, the derivative of $V_1(t)$ is negative definite

near the origin, hence the origin corresponds to a stable equilibrium point. It remains to show that the other equilibrium point corresponds to an unstable equilibrium point. To that purpose, consider the function

$$V_i(t) := \frac{1}{2} \|\mathbf{z}_i(t)\|^2 - \frac{1}{2} z_4^2(t),$$

where $\mathbf{z}_i(t) := \mathbf{z}_3(t) - \begin{bmatrix} -2V_d \\ 0 \end{bmatrix}$. With the control law (15), it is readily shown that the time derivative of $V_i(t)$ can be written as

$$\dot{V}_i(t) = V_d K_3 [[0 \ 1] \mathbf{z}_i(t)]^2 + K_4 z_4^2(t).$$

As in a neighborhood of $(\mathbf{z}_i = \mathbf{0}, z_4 = 0)$, one has that (i) $\dot{V}_i(t)$ is positive definite; (ii) $V_i(t)$ is not negative definite or negative semidefinite; and (iii) $V_i(t) = 0$ for $\mathbf{z}_i = \mathbf{0}, z_4 = 0$, it follows, from the Lyapunov's first instability theorem, that $(\mathbf{z}_i = \mathbf{0}, z_4 = 0)$ is an unstable equilibrium point, see, for example, [14]. This concludes the proof. \square

Next, it is shown that, with the proposed control law, the sway velocity also converges to zero. To that purpose, consider Figure 3, where the angle $\alpha(t)$ is the angle between the x -axis of the vehicle and the desired linear velocity, $\mathbf{v}_d(t)$, the angle $\alpha_1(t)$ is, as previously defined in Section 2.1, the angle between the x -axis of the vehicle and the desired final orientation, which is that of the vector $-\mathbf{S}(1)[\mathbf{t}_l(t) - \mathbf{t}_r(t)]^T$, and finally $\alpha_2(t)$ is the angle between the desired final orientation and the desired linear velocity, $\mathbf{v}_d(t)$, such that

$$\alpha(t) = \alpha_1(t) + \alpha_2(t) \tag{17}$$

holds for all t .

In order to show that the sway velocity $v(t)$ converges to zero, the sway dynamics will be considered together with that of $\alpha_1(t)$.

Before proceeding, notice that

$$\begin{cases} \cos[\alpha_1(t)] = [0 \ 1] \frac{\mathbf{t}_l(t) - \mathbf{t}_r(t)}{L_t} \\ \sin[\alpha_1(t)] = -[1 \ 0] \frac{\mathbf{t}_l(t) - \mathbf{t}_r(t)}{L_t} \end{cases} \tag{18}$$

and, using (7), (8), and (18), it is possible to rewrite (11) as

$$\omega_d(t) = \frac{2K_1 L_t}{1 + K_1^2 z_1^2(t)} \sin[\alpha_1(t)] [z_2(t) + V_d] - \frac{2K_1 L_t}{1 + K_1^2 z_1^2(t)} \cos[\alpha_1(t)] v(t) + K_3 [0 \ 1] \mathbf{z}_3(t). \tag{19}$$

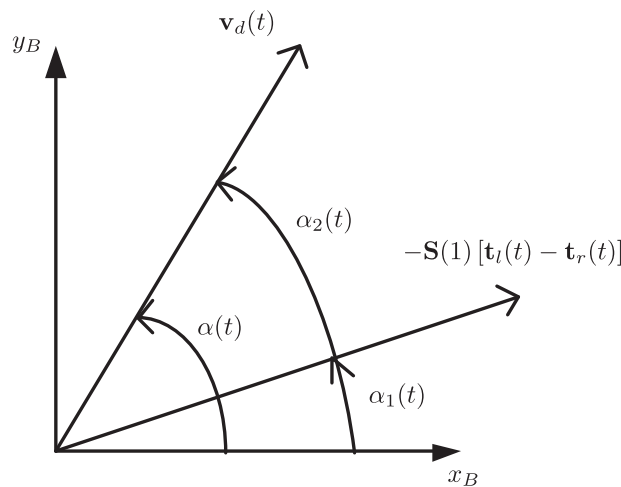


Figure 3. Angles $\alpha(t)$, $\alpha_1(t)$, and $\alpha_2(t)$.

Substituting (7) and (12) in (2) allows to write the sway dynamics as

$$\dot{v}(t) = -\frac{D_v + d_v[|v(t)|]}{M_v}v(t) - [z_2(t) + V_d][z_4(t) + \omega_d(t)]. \quad (20)$$

Substituting (19) in (20) allows to write

$$\dot{v}(t) = a_{11}(t)v(t) + a_{12}(t)\alpha_1(t) + u_v(t),$$

with

$$a_{11}(t) := -\frac{D_v + d_v[|v(t)|]}{M_v} + \frac{2K_1L_t}{1 + K_1^2z_1^2(t)}\cos[\alpha_1(t)][z_2(t) + V_d],$$

$$a_{12}(t) := -\frac{2K_1L_t}{1 + K_1^2z_1^2(t)}[z_2(t) + V_d]^2\text{sinc}[\alpha_1(t)],$$

and

$$u_v(t) := -[z_2(t) + V_d][z_4(t) + K_3[0 \ 1]\mathbf{z}_3(t)].$$

On the other hand, the derivative of $\alpha_1(t)$ is readily given by

$$\dot{\alpha}_1(t) = -\omega(t). \quad (21)$$

Substituting (12) in (21), and using (19), allows to write

$$\dot{\alpha}_1(t) = a_{21}(t)v(t) + a_{22}(t)\alpha_1(t) + u_{\alpha_1}(t),$$

with

$$a_{21}(t) := \frac{2K_1L_t}{1 + K_1^2z_1^2(t)}\cos[\alpha_1(t)],$$

$$a_{22}(t) := -\frac{2K_1L_t}{1 + K_1^2z_1^2(t)}[z_2(t) + V_d]\text{sinc}[\alpha_1(t)],$$

and

$$u_{\alpha_1}(t) := -z_4(t) - K_3[0 \ 1]\mathbf{z}_3(t).$$

Let

$$\mathbf{z}_5(t) := \begin{bmatrix} v(t) \\ \alpha_1(t) \end{bmatrix}.$$

In compact form, the dynamics of $\mathbf{z}_5(t)$ can be written, after straightforward computations, as

$$\dot{\mathbf{z}}_5(t) = \mathbf{A}(t)\mathbf{z}_5(t) + \mathbf{u}(t), \quad (22)$$

where

$$\mathbf{A}(t) := \begin{bmatrix} a_{11}(t) & a_{12}(t) \\ a_{21}(t) & a_{22}(t) \end{bmatrix}$$

and

$$\mathbf{u}(t) := [u_v(t) \ u_{\alpha_1}(t)]^T,$$

Notice that, in the definitions of $a_{12}(t)$ and $a_{22}(t)$ for $\alpha_1(t) = 0$, any finite value could have been chosen as it is multiplying by zero. The present choice, however, gives continuous functions.

Before presenting the main results of the section, the following proposition is introduced.

Proposition 2

Let the controller gain K_1 be chosen such that

$$0 < K_1 < \frac{D_v - \epsilon_1}{9L_t V_d} \quad (23)$$

for some arbitrarily small positive constant $\epsilon_1 > 0$. In the conditions of Proposition 1, if the error variable $\mathbf{z}_3(t)$ converges to zero, given arbitrarily small positive constants $\epsilon_s > 0$ and $\epsilon_v > 0$, then there exists $t_i \geq t_0$ such that

$$\begin{cases} \frac{2}{\pi} - \epsilon_s \leq \text{sinc}[\alpha_1(t)] \leq 1 \\ |z_2(t)| \leq \frac{1}{2}V_d \\ \frac{1}{2}V_d \leq |z_2(t) + V_d| \leq \frac{3}{2}V_d \\ |v(t)| \leq \frac{3}{4}V_d + \epsilon_v \end{cases} \quad (24)$$

for all $t \geq t_i$.

Proof

First, notice that, from the definition of $\alpha_2(t)$, it is easy to see that

$$\cos[\alpha_2(t)] = \frac{1}{V_d} \mathbf{v}_d(t) \cdot \left[-\mathbf{S}(1) \frac{\mathbf{t}_l(t) - \mathbf{t}_r(t)}{L_t} \right] = \frac{1}{\sqrt{1 + K_1^2 z_1^2(t)}} > 0,$$

which allows to conclude that

$$\alpha_2(t) \in]-\pi/2, \pi/2[. \quad (25)$$

On the other hand, in the conditions of Proposition 1, it is possible to conclude that when $\mathbf{z}_3(t)$ converges to zero, so does $\alpha(t)$. According to (17) and (25), this allows to conclude that, in the conditions of the Proposition, given any arbitrarily small positive constant $\epsilon_{\alpha_1} > 0$, it is possible to choose $t^* \geq t_0$ such that $|\alpha_1(t)| \leq \pi/2 + \epsilon_{\alpha_1}$ for all $t \geq t^*$. Therefore, given any arbitrarily small positive constant $\epsilon_s > 0$, it is possible to choose $t_1 \geq t_0$ such that the first inequality of (24) holds. As in the conditions of the proposition, $z_2(t)$ converges to zero exponentially fast, it is possible to choose $t_2 \geq t_1 \geq t_0$ such that the second inequality of (24) holds for $t \geq t_2$, which also immediately entails the third. To show the last inequality, consider the Lyapunov-like function $V_v(t) := \frac{1}{2}v^2(t)$. The time derivative of $V_v(t)$ is given by

$$\begin{aligned} \dot{V}_v(t) = & -\frac{D_v + d_v[|v(t)|]}{M_v} v^2(t) + \frac{2K_1 L_t}{1 + K_1^2 z_1^2(t)} \cos[\alpha_1(t)] [z_2(t) + V_d] v^2(t) \\ & + \left(-\frac{2K_1 L_t}{1 + K_1^2 z_1^2(t)} [z_2(t) + V_d]^2 \sin[\alpha_1(t)] + u_v(t) \right) v(t). \end{aligned}$$

As $d_v[|v(t)|] \geq 0$, and using simple inequalities, it is possible to write

$$\dot{V}_v(t) \leq -\frac{D_v}{M_v} v^2(t) + 2K_1 L_t |z_2(t) + V_d| v^2(t) + (2K_1 L_t |z_2(t) + V_d|^2 + |u_v(t)|) |v(t)|.$$

Now, for $t \geq t_2$, it is further possible to write

$$\dot{V}_v(t) \leq -\frac{D_v}{M_v} v^2(t) + 3K_1 L_t V_d v^2(t) + \left(\frac{9}{2} K_1 L_t V_d^2 + |u_v(t)| \right) |v(t)|.$$

Now, assuming (23), one gets

$$\dot{V}_v(t) \leq -\frac{2}{3} \frac{D_v}{M_v} v^2(t) + \frac{1}{2} \frac{D_v}{M_v} V_d |v(t)| + |u_v(t)| |v(t)|$$

for $t \geq t_2$. In the conditions of the proposition, $u_v(t)$ converges to zero. As such, given any arbitrarily positive small constant $\epsilon_v > 0$, there exists $t_3 \geq t_2 \geq t_0$ such that

$$|u_v(t)| \leq \frac{2}{3} \frac{D_v}{M_v} \epsilon_v$$

for all $t \geq t_3$ and as such it follows that

$$\dot{V}_v(t) \leq -\frac{2}{3} \frac{D_v}{M_v} v^2(t) + \frac{D_v}{M_v} \left(\frac{1}{2} V_d + \frac{2}{3} \epsilon_v \right) |v(t)|$$

for all $t \geq t_3$. But then notice that, for $t \geq t_3$ and

$$|v(t)| > \frac{3}{4} V_d + \epsilon_v,$$

it follows that $\dot{V}_v(t) < 0$. As such, there exists $t_4 \geq t_3$ such that

$$|v(t)| \leq \frac{3}{4} V_d + \epsilon_v.$$

This concludes the proof, as (24) holds for $t_i = t_4$. \square

The following theorem is the main result of this section.

Theorem 1

Consider an underactuated AUV moving in the horizontal plane in a mission scenario as described in Section 2.1, with kinematics and dynamics given by (1) and (2), respectively. Suppose that the conditions of Proposition 1 hold. Further assume that (23) is true and, in addition, the controller gain K_1 is chosen such that

$$\frac{D_v}{M_v} \frac{2K_1 L_t}{1 + K_1^2 Z_1^2} \frac{V_d}{2} \left(\frac{2}{\pi} - \epsilon_s \right) - (2K_1 L_t)^2 \left(\left(\frac{3}{2} V_d \right)^2 + \frac{1}{4} \left[\left(\frac{3}{2} V_d \right)^2 + 1 \right]^2 \right) \geq \epsilon_1 \quad (26)$$

is true, where Z_1 is a positive constant such that

$$K_1 Z_1 > \frac{3}{\sqrt{7}} \quad (27)$$

and ϵ_1 is an arbitrarily sufficiently small positive constant. Then, in the conditions of Proposition 1, if the error variable $\mathbf{z}_3(t)$ converges to zero, then the sway velocity $v(t)$ also converges to zero. Moreover, the error $z_1(t)$ converges to zero, hence solving the initial docking approach problem stated in Section 2.1 for almost all initial conditions.

Proof

The key idea of the proof is to show that, after some time, the nonlinear system (22) is input-to-state stable with respect to the input $\mathbf{u}(t)$, which allows to conclude that the sway velocity converges to zero and, as all the other variables also converge to zero, it follows that so does $z_1(t)$ as it is input-to-state stable with respect to the other variables. First, it is shown earlier that, after some time, $z_1(t)$ is necessarily bounded. Using Proposition 2, choose $t_i \geq t_0$ such that (24) holds for $t_i \geq t_0$ and consider the Lyapunov-like function

$$V_0(t) := \frac{1}{2} z_1^2(t).$$

Using (5), (7), and (8) it is possible to write

$$\dot{V}_0(t) \leq -\frac{2L_t V_d K_1}{\sqrt{1 + K_1^2 z_1^2(t)}} z_1^2(t) + 2L_t \left\| \begin{bmatrix} z_2(t) \\ z_3(t) \end{bmatrix} - \begin{bmatrix} z_2(t) \\ z_3(t) \end{bmatrix} + \begin{bmatrix} 0 \\ v(t) \end{bmatrix} \right\| |z_1(t)| \quad (28)$$

As in the conditions of the theorem, both $z_2(t)$ and $\mathbf{z}_3(t)$ converge to zero, and using (24), choosing an arbitrarily small positive constant $\epsilon_V > 0$, there exists $t_j \geq t_i$ such that

$$\left\| \begin{bmatrix} z_2(t) \\ z_3(t) \end{bmatrix} - \begin{bmatrix} z_2(t) \\ z_3(t) \end{bmatrix} + \begin{bmatrix} 0 \\ v(t) \end{bmatrix} \right\| \leq \frac{3}{4} V_d + \epsilon_V$$

for all $t \geq t_j$ and as such, it is possible to bound (28) by

$$\dot{V}_0 \leq -\frac{2L_t V_d K_1}{\sqrt{1 + K_1^2 z_1^2(t)}} z_1^2(t) + 2L_t \left(\frac{3}{4} V_d + \epsilon_V \right) |z_1(t)|$$

for all $t \geq t_j$. Now, notice that, choosing ϵ_V sufficiently small, and considering (27), if $|z_1(t)| > Z_1$, then for $t \geq t_j$, one has $\dot{V}_0(t) < 0$. But this implies that it is possible to chose $t_k \geq t_j$ such that $|z_1(t)| \leq Z_1$ for all $t \geq t_k$.

Next, it is shown that, for $t \geq t_k$, the nonlinear system (22) is input-to-state stable with respect to the input $\mathbf{u}(t)$. With that in mind, consider the Lyapunov-like function

$$V_2(t) = \frac{1}{2} \|\mathbf{z}_5(t)\|^2,$$

whose derivative is given by

$$\dot{V}_2(t) = \mathbf{z}_5^T(t) \mathbf{A}_s(t) \mathbf{z}_5(t) + \mathbf{z}_5^T(t) \mathbf{u}(t),$$

with

$$\mathbf{A}_s(t) := \frac{1}{2} [\mathbf{A}(t) + \mathbf{A}^T(t)].$$

If $\lambda_M[\mathbf{A}_s(t)] \leq L_M < 0$, where $\lambda_M(\mathbf{X})$ stands for the maximum eigenvalue of \mathbf{X} , it is trivially shown that the system is input-to-state with respect to $\mathbf{u}(t)$, see, for example, [14]. The characteristic polynomial of $\mathbf{A}_s(t)$ is given by

$$s[c(t)] = c^2(t) + c_1(t)c(t) + c_0(t),$$

with $c_1(t) := -a_{11}(t) - a_{22}(t)$ and $c_0(t) := a_{11}(t)a_{22}(t) - \frac{[a_{12}(t)+a_{21}(t)]^2}{4}$. If there exist $\epsilon_b > 0$ and $\epsilon_a > 0$ such that $c_1(t) > \epsilon_b$ and $c_0(t) > \epsilon_a$, then it follows that the nonlinear system (22) is input-to-state stable with respect to $\mathbf{u}(t)$. Expanding $c_1(t)$ and using simple inequalities, together with (24), allows to conclude that

$$c_1(t) \geq \frac{D_v}{M_v} - 3K_1 L_t V_d,$$

for all $t \geq t_k$. But then, with (23), it immediately follows that

$$c_1(t) \geq \frac{2}{3} \frac{D_v}{M_v}$$

for all $t \geq t_k$, which guarantees the existence of $\epsilon_b > 0$ such that $c_1(t) > \epsilon_b$ for $t \geq t_k$. Expanding $c_0(t)$ and using simple inequalities, coupled with (24), it is possible to conclude that

$$c_0(t) \geq \frac{D_v}{M_v} \frac{2K_1 L_t}{1 + K_1^2 Z_1^2} \frac{V_d}{2} \left(\frac{2}{\pi} - \epsilon_s \right) - (2K_1 L_t)^2 \left(\left(\frac{3}{2} V_d \right)^2 + \frac{1}{4} \left[\left(\frac{3}{2} V_d \right)^2 + 1 \right]^2 \right)$$

for $t \geq t_k$ and $\alpha_1(t) \neq 0$, which is also trivially shown to hold for $\alpha_1(t) = 0$. But then, if (26) is true, it follows that there exists $\epsilon_a > 0$ such that $c_a(t) > \epsilon_a$ for $t \geq t_k$. This allows to conclude that the nonlinear system (22) is input-to-state stable with respect to $\mathbf{u}(t)$. As $\mathbf{u}(t)$ converges to zero in the conditions of the theorem, it follows that the sway velocity $v(t)$ converges to zero and, as the dynamics of $z_1(t)$ are also tribally shown to be input-to-state stable with respect to $v(t)$, $z_2(t)$, and $\mathbf{z}_3(t)$, it follows that $z_1(t)$ converges to zero, hence concluding the proof. \square

Remark 1

At this point, it is important to remark that the conditions that are presented here are only sufficient. In practice, larger values of K_1 may still yield controllers that solve the initial docking problem as stated in Section 2.1.

Remark 2

The analysis of stability presented here has some similarities with that presented in [12]. However, the desired velocity that is considered in the present paper is bounded, whereas in [12], it could be arbitrarily large, depending on the initial error. As such, the stability analysis presented herein is much more intricate, as previously detailed.

Remark 3

In spite of the rather cumbersome stability analysis, notice that the resulting control law is quite simple, designed in body-fixed coordinates, and requiring few sensors. In particular, the control law only requires the linear and angular velocities of the vehicle and the positions of the transponders with respect to the vehicle, all expressed in body-fixed coordinates, as they are usually available from the USBL sensor installed in the AUV.

Remark 4

The problem is set in this paper in the horizontal plane, as the docking maneuver is usually performed at constant depth and independent depth controllers usually stabilize the AUV. Nevertheless, the control law could be extended to 3D, only the analysis results much more intricate. Considering this control law, at constant depth, the heave velocity should be zero. If not, its effect should be similar to that of the surge speed and could hence be accounted for during the design and stability analysis in a similar way to that of the surge velocity.

3.2. Final docking approach

This section details the design and stability analysis of an adaptive control law for the final docking approach of an AUV, as defined in Section 2.2. The goal here is to drive the lateral error, $l_y(t)$, and the orientation error, $\alpha_1(t)$, to zero, whereas the longitudinal distance $l_x(t)$ follows a predefined profile.

The longitudinal distance is defined as

$$l_x(t) := - \left[\frac{\mathbf{t}_l(t) + \mathbf{t}_r(t)}{2} \right]^T \left[\mathbf{S}(1) \frac{\mathbf{t}_l(t) - \mathbf{t}_r(t)}{L_t} \right] = \frac{1}{L_t} \mathbf{t}_l^T(t) \mathbf{S}(1) \mathbf{t}_r(t).$$

The lateral error is defined as

$$l_y(t) := \left[\frac{\mathbf{t}_l(t) + \mathbf{t}_r(t)}{2} \right]^T \frac{\mathbf{t}_l(t) - \mathbf{t}_r(t)}{L_t} = \frac{\|\mathbf{t}_l(t)\|^2 - \|\mathbf{t}_r(t)\|^2}{2L_t}.$$

The orientation error $\alpha_1(t)$ is as defined in Section 2.1, whose derivative is $\dot{\alpha}_1(t) = -\omega(t)$. After some rather straightforward computations, it is possible to write the derivatives of $l_x(t)$ and $l_y(t)$, in compact form, as

$$\begin{bmatrix} \dot{l}_x(t) \\ \dot{l}_y(t) \end{bmatrix} = -\mathbf{R}_{\alpha_1}(t) \mathbf{v}(t),$$

where $\mathbf{R}_{\alpha_1}(t)$ is the rotation matrix

$$\mathbf{R}_{\alpha_1}(t) = \begin{bmatrix} \cos[\alpha_1(t)] & \sin[\alpha_1(t)] \\ -\sin[\alpha_1(t)] & \cos[\alpha_1(t)] \end{bmatrix}.$$

Let $\mathbf{l}(t) := [l_x(t) \ l_y(t)]^T$ and define the error variable

$$\mathbf{z}_6(t) := \mathbf{l}(t) - \mathbf{l}_d(t),$$

with $\mathbf{l}_d(t) := [l_{xd}(t) \ 0]$. Define also the error variable

$$z_7(t) := \alpha_1(t)$$

and consider the Lyapunov candidate function

$$V_3(t) := \frac{1}{2} \|\mathbf{z}_6(t)\|^2 + \frac{1}{2} z_7^2(t).$$

The time derivative of $V_3(t)$ is given by

$$\dot{V}_3(t) = -\mathbf{z}_6^T(t) \left[\mathbf{R}_{\alpha_1}(t) \mathbf{v}(t) + \dot{\mathbf{i}}_d(t) \right] - z_7(t) \omega(t).$$

Setting $\mathbf{v}(t)$ and $\omega(t)$ equal to

$$\mathbf{v}_{d2}(t) := -\mathbf{R}_{\alpha_1}^T(t) \left[\dot{\mathbf{i}}_d(t) - K_5 \mathbf{z}_6(t) \right]$$

and

$$\omega_{d2}(t) := K_6 z_7(t),$$

respectively, where K_5 and K_6 are positive constant control gains, results in a negative definite derivative of $V_3(t)$. As $\mathbf{v}(t)$ and $\omega(t)$ are not actual control variables, and following the standard backstepping technique, consider the error variables

$$\mathbf{z}_8(t) := \mathbf{v}(t) - \mathbf{v}_{d2}(t),$$

$$z_9(t) := \omega(t) - \omega_{d2}(t),$$

and define the augmented Lyapunov function

$$V_4(t) := V_3(t) + \frac{1}{2} \|\mathbf{z}_8(t)\|^2 + \frac{1}{2} z_9^2(t).$$

Setting

$$\tau_{\mathbf{v}}(t) = \mathbf{S}[\omega(t)] \mathbf{M} \mathbf{v}(t) + \boldsymbol{\phi}_{\mathbf{v}}^T[\mathbf{v}(t)] \hat{\boldsymbol{\psi}}_{\mathbf{v}}(t) + \mathbf{M}[\dot{\mathbf{v}}_{d2}(t) + \mathbf{R}_{\alpha_1}^T(t) \mathbf{z}_6(t) - K_7 \mathbf{z}_8(t)] \quad (29)$$

and

$$\tau_{\omega}(t) = \boldsymbol{\phi}_{\omega}[\omega(t)]^T \hat{\boldsymbol{\psi}}_{\omega}(t) + J[\dot{\omega}_{d2}(t) + z_7(t) - K_8 z_9(t)], \quad (30)$$

where K_7 and K_8 are positive constant control gains and $\hat{\boldsymbol{\psi}}_{\mathbf{v}}(t)$ and $\hat{\boldsymbol{\psi}}_{\omega}(t)$ are estimates of $\boldsymbol{\psi}_{\mathbf{v}}$ and $\boldsymbol{\psi}_{\omega}$, respectively, allows to write

$$\begin{aligned} \dot{V}_4(t) = & -K_5 \|\mathbf{z}_6\|^2 - K_6 z_7^2(t) - K_7 \|\mathbf{z}_8(t)\|^2 - K_8 z_9^2(t) \\ & - \mathbf{z}_8^T(t) \mathbf{M}^{-1} \boldsymbol{\phi}_{\mathbf{v}}^T[\mathbf{v}(t)] [\boldsymbol{\psi}_{\mathbf{v}} - \hat{\boldsymbol{\psi}}_{\mathbf{v}}] - \frac{1}{J} z_9(t) \boldsymbol{\phi}_{\omega}[\omega(t)]^T [\boldsymbol{\psi}_{\omega} - \hat{\boldsymbol{\psi}}_{\omega}]. \end{aligned}$$

In order to design an adaptive control law, let $\tilde{\boldsymbol{\psi}}_{\mathbf{v}}(t) := \boldsymbol{\psi}_{\mathbf{v}} - \hat{\boldsymbol{\psi}}_{\mathbf{v}}(t)$ and $\tilde{\boldsymbol{\psi}}_{\omega}(t) := \boldsymbol{\psi}_{\omega} - \hat{\boldsymbol{\psi}}_{\omega}(t)$ denote the estimation errors of $\hat{\boldsymbol{\psi}}_{\mathbf{v}}(t)$ and $\hat{\boldsymbol{\psi}}_{\omega}(t)$, respectively, and consider the augmented Lyapunov candidate function

$$V_5(t) := V_4(t) + \frac{1}{2} \|\tilde{\boldsymbol{\psi}}_{\mathbf{v}}(t)\|^2 + \frac{1}{2} \|\tilde{\boldsymbol{\psi}}_{\omega}(t)\|^2.$$

With the estimation laws

$$\dot{\hat{\boldsymbol{\psi}}}_{\mathbf{v}}(t) = -\boldsymbol{\phi}_{\mathbf{v}}[\mathbf{v}(t)] \mathbf{M}^{-1} \mathbf{z}_8(t) \quad (31)$$

and

$$\dot{\hat{\boldsymbol{\psi}}}_{\omega}(t) = -\frac{1}{J} z_9(t) \boldsymbol{\phi}_{\omega}[\omega(t)] \quad (32)$$

the derivative of $V_5(t)$ results in

$$\dot{V}_5(t) = -K_5 \|\mathbf{z}_6\|^2 - K_6 z_7^2(t) - K_7 \|\mathbf{z}_8(t)\|^2 - K_8 z_9^2(t), \quad (33)$$

which is negative semidefinite. The following theorem is the main result of this section.

Theorem 2

Consider a fully actuated AUV moving in the horizontal plane in a mission scenario as described in Section 2.2, with kinematics and dynamics given by (1) and (3), respectively. Then, with the adaptive control law (29), (30), (31), and (32), where $K_5, K_6, K_7,$ and K_8 are positive constant control gains, the error variables $\mathbf{z}_6(t), z_7(t), \mathbf{z}_8(t)$ and $z_9(t)$ converge to zero, hence solving the problem of final docking approach stated in Section 2.2.

Proof

First, notice that $V_5(t)$ is positive definite and radially unbounded. Moreover, under the conditions of the theorem, the derivative of $V_5(t)$, given by (33), is negative semidefinite, which allows to conclude that $V_5(t)$ approaches its own limit and $V_5(t) \leq V_5(t_0)$ for all $t \geq t_0$ which, in turn, allows to conclude that all error variables $\mathbf{z}_6(t), z_7(t), \mathbf{z}_8(t)$ and $z_9(t), \tilde{\psi}_v(t),$ and $\tilde{\psi}_\omega(t)$ are bounded. Computing the second derivative of $V_5(t)$, and using the fact that all error variables are bounded, immediately allows to conclude that $\dot{V}_5(t)$ is also bounded, which implies that $\ddot{V}_5(t)$ is uniformly continuous. But then, as $V_5(t)$ has a finite limit and $\dot{V}_5(t)$ is uniformly continuous, it follows from the Barbalat’s Lemma that $\dot{V}_5(t)$ converges to zero, thus concluding the proof. \square

Remark 5

Similarly to the initial docking step, the control law proposed in the final docking control approach could be extended to 3D. The stability analysis remains unchanged.

Remark 6

It is important to stress that Theorem 2 ensures that the appropriate error variables converge to zero, but it does not provide converge speeds. Hence, in order to ensure appropriate docking behavior and avoid collision with the docking station, simulations must be carried out to tune the controller gains so that the resulting trajectories are adequate. This is a common solution in nonlinear control problems.

4. SIMULATION RESULTS

To illustrate the performance of the proposed integrated guidance and control law, computer simulations are presented in this section. In the simulations a simplified model of the SIRENE vehicle was employed, assuming that the vehicle is directly actuated in force and torque; see [15]. The parameters of the vehicle are detailed in Table I, with $d_u[|u(t)|] = D_{u|u}|u(t)|, d_v[|v(t)|] = D_{v|v}|v(t)|$ and $d_\omega[|\omega(t)|] = D_{\omega|\omega}|\omega(t)|$.

The initial position of the vehicle is $\mathbf{p}_0 = [-100 \ 10]^T$ (m), its initial yaw is 150° , its initial linear velocity is $\mathbf{v}_0 = [1 \ 0]^T$ m/s, and its initial angular velocity is $\omega_0 = 0$ °/s. The positions of the left and right transponders, in the inertial frame, are $\mathbf{t}_l = [1 \ 0]^T$ and $\mathbf{t}_r = [-1 \ 0]^T$, respectively. The controller parameters were tuned in order to achieve an interesting trajectory, and were thus set to $K_1 = 0.01, K_2 = 0.2, K_3 = 0.1, K_4 = 2, K_5 = 0.025, K_6 = 0.5, K_7 = 2,$ and $K_8 = 0.5$. The controller switches to the second stage when the distance between the vehicle and the docking position reaches 25 m, and it stops when this distance reaches 0.5 m. For the second control law, the initial estimates of the hydrodynamic parameters were set with offsets of around 10% of the nominal value. Finally, control saturation was also considered in order to see that effect in the overall performance of the proposed strategy. The maximum allowed force is 500 N along the surge axis, 100 N along the sway axis, and the maximum allowed torque was set to 1500 Nm.

Table I. Vehicle parameters.

Parameter	Value	Parameter	Value	Parameter	Value
M_u (Kg)	2234.5	D_u (Kg/s)	0	$D_{u u}$ (Kg/m)	35.4090
M_v (Kg)	2234.5	D_v (Kg/s)	346	$D_{v v}$ (Kg/m)	667.5552
J (Kg m ²)	2000	D_ω (Kg m ² /s)	1427.2	$D_{\omega \omega}$ (Kg m ²)	26036

The evolution of the trajectory described by the vehicle is depicted in Figure 4, where the positions of the transponders are marked with red crosses, whereas the evolution of the linear and angular velocity is shown in Figure 5. The control inputs are plotted in Figure 6, while the evolution of the error variables is depicted in Figure 7.

As it is possible to observe, the vehicle describes a smooth trajectory and the desired behavior is achieved. The controller switches to the final docking scenario at $t = 62.37$ s. The speed profile is as desired and the error variables converge to zero.

In order to evaluate the performance of the proposed strategy in the presence of sensor noise, the previous simulation was modified and sensor noise was included for all sensors. In particular, the USBL measurements are assumed to be corrupted by additive zero-mean white Gaussian noise, with standard deviation of 1 m, whereas the linear and angular velocity measurements are assumed to be corrupted by additive zero-mean white Gaussian noise, with standard deviation of 0.1 m/s and $0.5^\circ/\text{s}$, respectively. An additional first order, low-pass filter was included in the actuation of the vehicle for the second stage in order to minimize the effect of sensor noise, with unit gain and cut-off frequency of 1 rad/s. The evolution of the trajectory described by the vehicle is depicted in Figure 8, where the positions of the transponders are marked with red crosses, while the evolution of the linear and angular velocity is shown in Figure 9. The control inputs are plotted in Figure 10, whereas the evolution of the error variables is depicted in Figure 11.

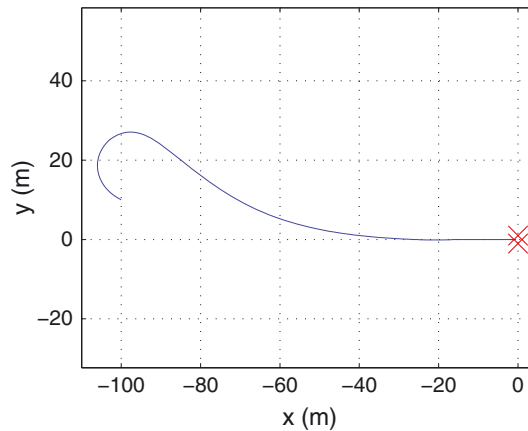


Figure 4. Trajectory described by the vehicle.

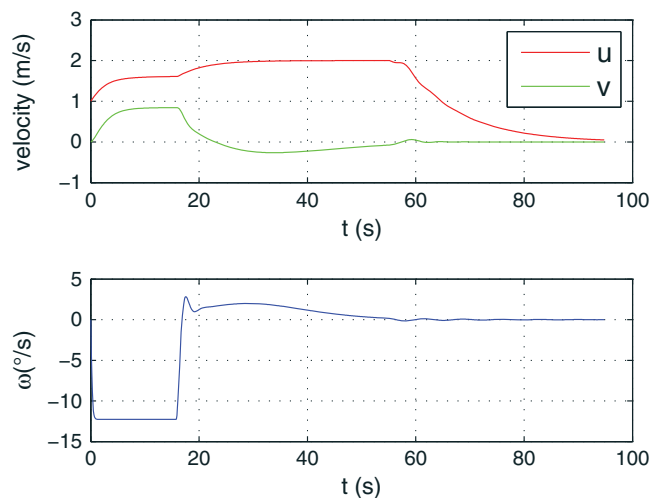


Figure 5. Evolution of the velocity of the vehicle.

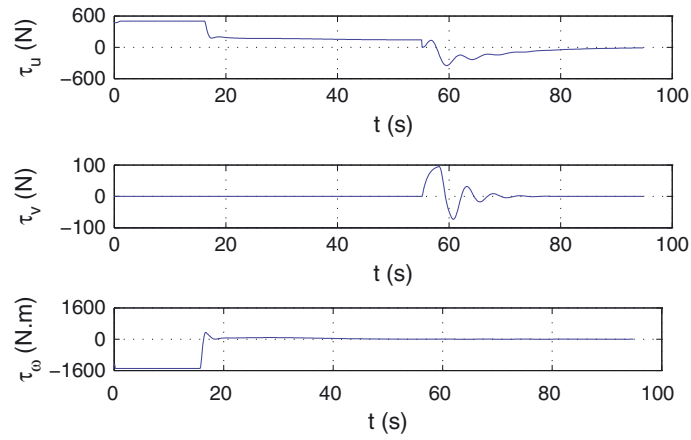


Figure 6. Evolution of the control inputs.

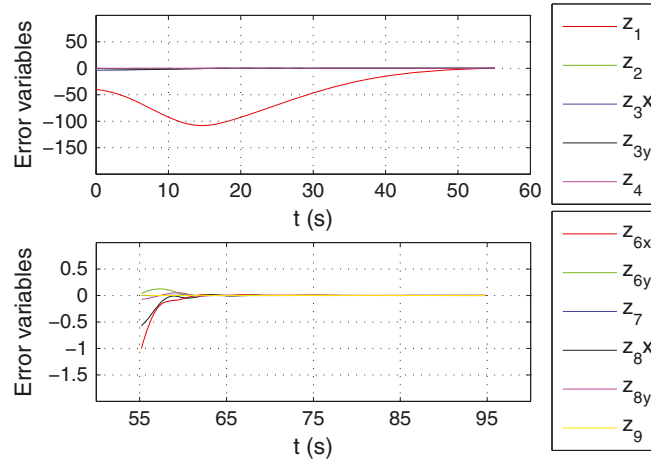


Figure 7. Evolution of the error variables.

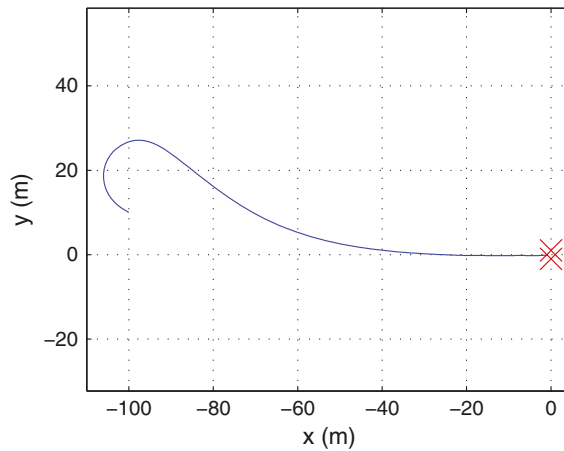


Figure 8. Trajectory described by the vehicle in the presence of sensor noise.

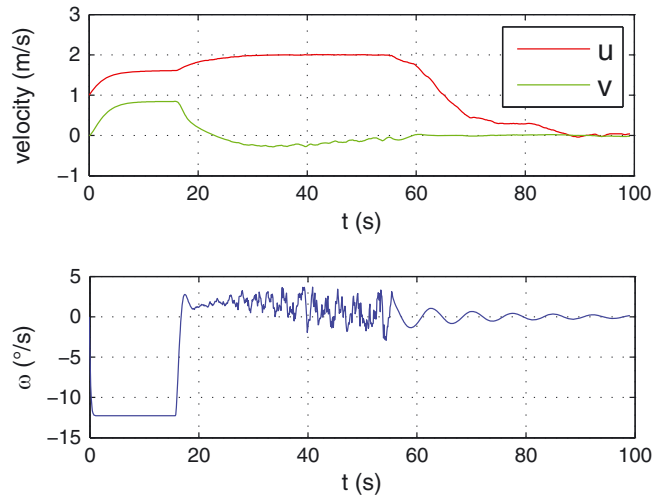


Figure 9. Evolution of the velocity of the vehicle in the presence of sensor noise.

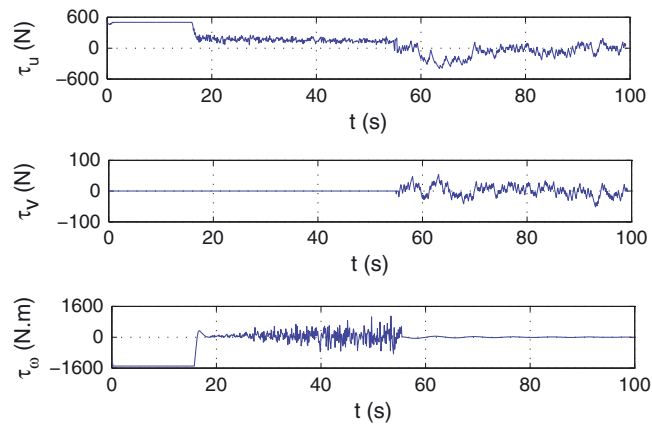


Figure 10. Evolution of the control inputs in the presence of sensor noise.

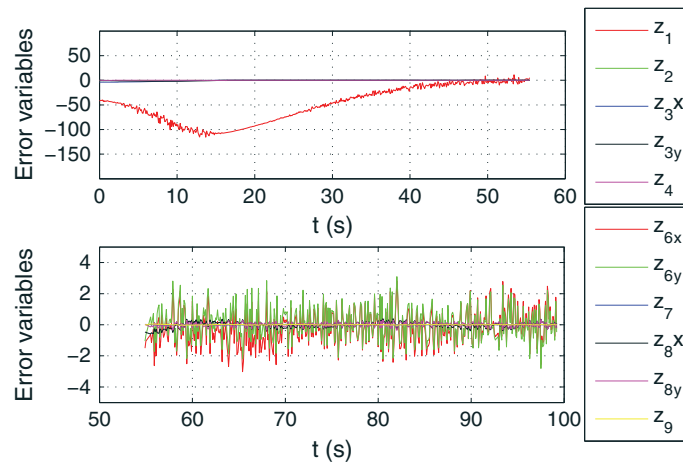


Figure 11. Evolution of the error variables in the presence of sensor noise.

The most distinct difference between these plots and those obtained without sensor noise is the effect of the sensor noise in the actuation. However, the trajectory and speed profiles are very similar. Naturally, the error variables are now noisy. Overall, the controller solves the problem, with good performance, under the presence of both sensor noise and uncertainty in the hydrodynamic damping parameters.

5. CONCLUSIONS

This paper presented a novel integrated guidance and control law to solve the docking problem of an autonomous underwater vehicle. The control approach was divided into two steps, one farther away from the base and another in the close proximity in order to better explore the configuration of the AUV. In the first case, convergence to zero of the appropriate error variables was shown for almost all initial conditions, whereas in the second case, this is shown for all initial conditions. In addition, uncertainty in the hydrodynamic parameters was considered and explicitly addressed, with an adaptive control law, in the final approach to the base. Simulation results evidence good performance of the controller in the presence of both sensor noise, uncertainty in the hydrodynamic damping parameters and control saturation.

Although the docking maneuver should be done in the best possible conditions, preferably without ocean currents, it is possible to explicitly take this into account in the controller design. As a result, the heading of the vehicle in the first step is adjusted as to counteract the ocean currents, while in the second step direct actuation is used on each axis. In practice, the best approach would still be to seek docking in the opposite direction of the currents, which would only result in a higher control demand along the surge axis.

ACKNOWLEDGEMENTS

This work was partially supported by the FCT (PEst-OE/EEI/LA0009/2013) and by the EU Project TRIDENT (Contract No. 248497).

REFERENCES

- Batista P, Silvestre C, Oliveira P. A sensor based controller for homing of underactuated AUVs. *IEEE Transactions on Robotics* 2009; **25**(3):701–716.
- Batista P, Silvestre C, Oliveira P. A time differences of arrival based homing strategy for autonomous underwater vehicles. *International Journal of Robust and Nonlinear Control* 2010; **20**(15):1758–1773.
- Cowen S, Briest S, Dombrowski J. Underwater docking of autonomous undersea vehicles using optical terminal guidance. *Proceedings of the MTS/IEEE OCEANS 97*, vol. 2, Halifax, Canada, 1997; 1143–1147.
- Feezor M, Sorrell F, Blankinship P, Bellingham J. Autonomous underwater vehicle homing/docking via electromagnetic guidance. *IEEE Journal of Oceanic Engineering* 2001; **26**(4):515–521.
- Lee, PM, Jeon, BH, Kim SM. Visual servoing for underwater docking of an autonomous underwater vehicle with one camera. *Proceedings of the 2003 OCEANS*, vol. 2, 2003; 677–682.
- Park, JY, Jun, HH, Lee, PM, Lee, FY, Oh, JH. Experiment on underwater docking of an autonomous underwater vehicle 'ISiMI' using optical terminal guidance. *Proceedings of the OCEANS 2007*, vol. 2, Vancouver, BC, Canada, 2007; 1–6.
- Jantapremjit P, Wilson P. Control and guidance for homing and docking tasks using an autonomous underwater vehicle. *Proceedings of the IEEE/RSJ International Conference on Intelligent Robots and Systems*, San Diego, CA, USA, 2007; 3672–3677.
- Batista P, Silvestre C, Oliveira P. A two-step control strategy for docking of autonomous underwater vehicles. *Proceedings of the 2012 American Control Conference*, Montréal, Canada, 2012; 5395–5400.
- Fossen T. *Guidance and Control of Ocean Vehicles*. Wiley: Chichester, UK, 1994.
- Repoulas F, Papadopoulos E. Planar trajectory planning and tracking control design for underactuated AUVs. *Ocean Engineering* 2007; **34**(11-12):1650–1667.
- Almeida J, Silvestre C, Pascoal A. Cooperative control of multiple surface vessels in the presence of ocean currents and parametric model uncertainty. *International Journal of Robust Nonlinear Control* 2010; **20**(14):1549–1565.
- Indiveri G, Aicardi M, Casalino G. Nonlinear time-invariant feedback Control of an underactuated marine vehicle along a straight course. *Proceedings of the 5th IFAC Conference on Manoeuvring and Control of Marine Craft*, Aalborg, Denmark, August 2000; 221–226.

13. Pedone P, Zizzari A, Indiveri G. Path-following for the dynamic model of a marine surface vessel without closed-loop control of the surge speed. *Proceedings of the 8th IFAC Conference on Control Applications in Marine Systems*, Rostock, Germany, 2010; 243–248.
14. Khalil H. *Nonlinear Systems* (3rd edn.) Prentice Hall: New Jersey, USA, 2001.
15. Silvestre C, Aguiar A, Oliveira P, Pascoal A. Control of the SIRENE underwater shuttle: system design and tests at sea. *Proceedings of the 17th International Conference on Offshore Mechanics and Arctic Engineering*, Lisbon, Portugal, 1998.